nanocrystals might pack into two-dimensional arrays. Such samples would be of great interest in the study of interparticle phenomena.

Acknowledgment. This work was supported by the Director, Office of Energy Research, Office of Basic Energy Sciences, Division of Materials Sciences, of the U.S. Department of Energy, under Contract No. DE-AC03-76SF0098. V.L.C. acknowledges IBM for a predoctoral fellowship. We thank Professor Marcin Majda, Dr. C. Goss, and other members of the Majda group for their assistance in making SAMs. We thank the XPS and RBS facilities of the Lawrence Berkeley Laboratory for use of the facilities. We thank the National Center for Electron Microscopy for use of the TEMs and digitizing facilities. Finally, we thank our colleague Dr. James Tobin of Lawrence Livermore National Lab for his collaborative work on ultraviolet photoemission studies of the nanocrystals.

Registry No. Gold, 7440-57-5; aluminum, 7429-90-5; cadmium sulfide, 1306-23-6; 1,6-hexanedithiol, 1191-43-1; 2-mercaptoacetic acid, 68-11-1.

Palladium Catalysis of O_2 Reduction by Electrons Accumulated on TiO_2 Particles during Photoassisted Oxidation of Organic Compounds

Chong-Mou Wang, Adam Heller,* and Heinz Gerischer*,[†]

Contribution from the Department of Chemical Engineering, The University of Texas at Austin, Austin, Texas 78712-1062. *Received December 2, 1991*

Abstract: Our earlier theoretical analysis suggested that the quantum efficiency of photoassisted oxidation of organic compounds in water by O_2 on n-TiO_2 surfaces can be limited by the kinetics of the reduction of O_2. When the rate of O_2 reduction is not sufficiently fast to match the rate of reaction of holes, an excess of electrons will accumulate on the TiO_2 particles, and the rate of electron–hole recombination will increase. We now show experimentally that electrons do indeed accumulate on slurried TiO_2 particles during photoassisted oxidation of 1.6 M aqueous methanol and that electrons on the slurried particles persist for at least ~1 min even in O_2-saturated solutions. The rate of particle depolarization, i.e. of electron transfer to dissolved O_2, is increased and the negative charge on the TiO_2 particles is completely eliminated upon incorporation of Pd^0 in the surface of the TiO_2 particles. We also show that incorporation of Pd^0 in the surface increases the quantum efficiency of the photoassisted oxidation of 10^{-2} M aqueous 2,2-dichloropropionate 3-fold at 0.01 wt % Pd and 7-fold at 2 wt % Pd.

Introduction

Photoassisted oxidation of organic contaminants of water[1-15] is of interest in the context of improving the quality of water and photosolubilization of oil slicks on seawater[16] for subsequent rapid bacterial degradation.[17] Similarly, photoassisted oxidation of organic contaminants of humid air on TiO_2 is being explored. TiO_2, whether anatase or rutile, is, because of its stability and in spite of the poor overlap of its excitation spectrum and the solar spectrum, the preferred photocatalyst. The reaction catalyzed involves oxidation of surface-adsorbed water by holes to produce OH radicals that oxidize organic compounds.[18] This reaction is coupled with reduction of dissolved O_2 initially to peroxide and ultimately to water. At high concentrations of organic reagents and at high irradiance, the rate of the hole-initiated oxidation can be fast, but it cannot be faster than the rate of O_2 reduction by electrons.[19,20] When O_2 is not reduced at a sufficiently high rate, electrons accumulate on the photocatalyst and the rate of radiationless electron–hole recombination is enhanced until the sum of the rates of recombination and electron transfer to oxygen equals the rate of photogeneration of holes. In this case, the rate of photooxidation equals, and is limited by, the rate of O_2 reduction.

In our earlier theoretical analyses,[19,20] we estimated the light flux and particle size where the quantum efficiency in a TiO_2 particle slurry becomes O_2 reduction rate limited. We predicted this to be the case when the particles do not have a particularly high density of shallow, near-surface electron traps to assist in the O_2 reduction process. Whether such traps are present or not, but particularly in the absence of a high density of such traps, modification of the surface by a catalyst for O_2 reduction, for example by group VIII metals, should increase the quantum efficiency of photoassisted oxidation in photocatalyst slurries. Pt incorporation[21] in photocatalysts has been extensively studied in the past in the context of catalysis of H_2 photoproduction, but few authors considered its role in O_2 reduction in photoassisted oxidation reactions. However, Izumi et al.[1] did point out that, in the photoassisted oxidation of hydrocarbons on TiO_2 powders, the Pt cocatalyst provides a site for more efficient utilization of photogenerated electrons in the reduction of O_2. Furthermore,

---

[†] Permanent address: Fritz-Haber-Institut der Max-Planck-Gesellschaft, Faradayweg 4-6, D-W-1000, Berlin 33, Germany.

(1) Izumi, I.; Dunn, W. W.; Wilbourn, K. O.; Fan, F. R.; Bard, A. J. *J. Phys. Chem.* **1980**, *84*, 3207.

(2) Hashimoto, K.; Kawai, T.; Sakata, T. *J. Phys. Chem.* **1984**, *88*, 4083.

(3) Ollis, D. F.; Turchi, C. *Environ. Prog.* **1990**, *9*, 229.

(4) Turchi, C. S.; Ollis, D. F. *J. Catal.* **1990**, *122*, 178.

(5) Matthews, R. W. *Aust. J. Chem.* **1987**, *40*, 667.

(6) Matthews, R. W. *J. Catal.* **1988**, *111*, 264.

(7) Matthews, R. W. *Water Res.* **1990**, *24*, 653.

(8) Kormann, C.; Bahnemann, D. W.; Hoffmann, M. R. *Environ. Sci. Technol.* **1991**, *25*, 494.

(9) Al-Ekabi, H.; Serpone, N. *J. Phys. Chem.* **1988**, *92*, 5726.

(10) Pelizzetti, E.; Borgarello, M.; Minera, C.; Pramauro, E.; Borgarello, E.; Serpone, N. *Chemosphere* **1988**, *17*, 499.

(11) Barbeni, M.; Morello, M.; Pramauro, E.; Pelizzetti, E.; Vincenti, M.; Borgarello, E.; Serpone, N. *Chemosphere* **1987**, *16*, 1165.

(12) Barbeni, M.; Pramauro, E.; Pelizzetti, E.; Borgarello, E.; Serpone, N. *Chemosphere* **1985**, *14*, 195.

(13) Barbeni, M.; Pramauro, E.; Pelizzetti, E.; Borgarello, E.; Graetzel, M.; Serpone, N. *Nouv. J. Chim.* **1984**, *8*, 547.

(14) Carey, J. H.; Oliver, B. G. *Water Pollut. Res. J. Can.* **1980**, *15*, 157.

(15) Fujihira, M.; Satoh, Y.; Osa, T. *J. Electroanal. Chem. Interfacial Electrochem.* **1981**, *126*, 277.

(16) Jackson, N. B.; Wang, C. M.; Luo, Z.; Schwitzgebel, J.; Ekerdt, J. G.; Brock, J. R.; Heller, A. *J. Electrochem. Soc.* **1991**, *138*, 3660.

(17) Carey, J. H.; Oliver, B. G. *Water Pollut. Res. J. Can.* **1980**, *15*, 157.

(18) Jaeger, C. D.; Bard, A. J. *J. Phys. Chem.* **1979**, *83*, 3146.

(19) Gerischer, H.; Heller, A. *J. Phys. Chem.* **1991**, *95*, 5261.

(20) Gerischer, H.; Heller, A. *J. Electrochem. Soc.* **1992**, *139*, 113.

(21) Kraeutler, B.; Bard, A. J. *J. Am. Chem. Soc.* **1978**, *100*, 4317.

0002-7863/92/1514-5230$03.00/0

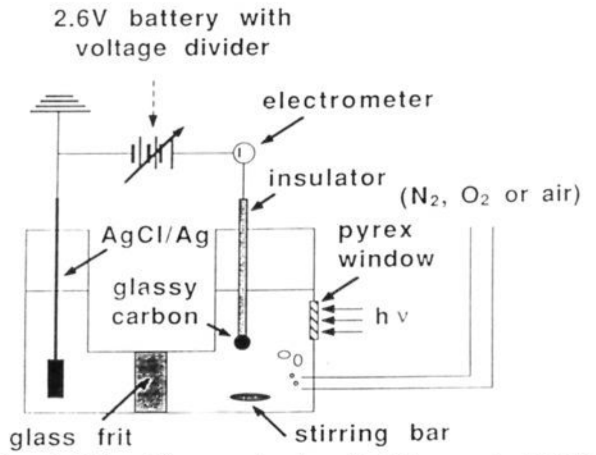

Figure 1. Cell used for measuring the residual charge on slurried TiO_2 and Pd-activated TiO_2 particles following illumination. Because the illuminated compartment contains an optically dense TiO_2 slurry, the particles are excited only near the window. The glassy-carbon electrode in the dark back of the illuminated compartment measures the charge of the particles after they traverse the ~2-cm front to back distance.

Kobayashi, Yoneyama, and Tamura showed[22] that, in the absence of organics, Pt films on TiO_2 monocrystals substantially enhance O_2 reduction. Here we show that the efficiency of the photoassisted oxidation of organic solutes (1.6 M methanol and 10^{-2} M 2,2-dichloropropionate) in water by dissolved O_2 is limited by the rate of electron transfer from the TiO_2 particles to O_2, that even in O_2-saturated solutions the electrons stay on the TiO_2 particles for at least ~1 min, that the particles are rapidly depolarized if partially coated with Pd, and that the quantum efficiency of photoassisted oxidation of organics by O_2 is increased when the TiO_2 particles are Pd activated.

Experimental Section

Slurry Cells. Two cells were used, one for the methanol oxidation experiments and the other for the sodium dichloropropionate oxidation experiments. Both cells were designed to allow control of the atmosphere. The cell used for the methanol experiments (Figure 1) had two compartments separated by a fine glass frit. The cell was designed so that the particles in the slurry, illuminated at the window in the front of one compartment, had to travel for >1 s and cover a distance of ~2 cm in order to discharge their excess charge at a vitreous-carbon electrode in the back of the same compartment, where the UV flux was negligible. Vitreous carbon was chosen for charge collection because of its inertness in both oxidation of methanol and reduction of oxygen or water in the potential range where TiO_2 particles can exchange electrons with it. The charge-collecting glassy-carbon electrode (Atomergic) was of 0.3-cm diameter and 0.65-cm length. Contact to it was made with a silver epoxy to a copper wire. The Ag/AgCl electrode in the second compartment consisted of a 0.1-cm-thick 1 × 2 cm^2 silver foil. Before each measurement, the Ag/AgCl electrode was cleaned in concentrated NH_4OH and reanodized in 1 M HCl and its −(0.040–0.045)-V potential vs SCE was confirmed. The TiO_2 slurry in the illuminated compartment was magnetically stirred and purged with N_2 (99.9%), O_2 (99.9%), or air for 30 min before each measurement. The slurry consisted of 5 mg of TiO_2 or Pd/TiO_2, 75 mL of water or an NaCl solution in water, and 5 mL of methanol. Prior to introduction into the test chamber, 40 mL of the slurry was sonicated (Bransonic ultrasonic cleaner, Aldrich) for 5 min. This 40-mL portion was poured into the illuminated compartment, while the remaining 35-mL portion was poured into the second compartment, containing the Ag/AgCl electrode. The front of the illuminated compartment, having the glassy-carbon electrode in its dark back, was illuminated using a 500-W Hg lamp (Oriel), the light of which was passed through a 10-cm-thick water filter and through an Oriel Model 53410 narrow-band interference filter with a transmission maximum at 360 and a bandwidth at half-peak of 10 nm. The area of the Pyrex window through which the cell was illuminated was 3.75 cm^2, and the UV (λ <400 nm) irradiance on the window was 0.5 mW cm^{-2}, corresponding, for 3.5-eV photons, to 5.3×10^{-6} einstein cm^{-2} h^{-1} and, for the 3.75-cm^2 window, to 2×10^{-5} einstein h^{-1}.

The electronics consisted of a regulated power supply (Lambda Electronics, Melville, NY), mercury batteries (2.3 V) with a homemade voltage divider, a Keithley 614 electrometer, and a Kipp and Zonen BD91 XYY′t recorder.

The second cell, in which the experiments with sodium dichloropropionate were performed, was a 2.5 × 2.5 × 5 cm^3 Pyrex cuvette with a magnetic stirrer and an attached 100-mL bulb containing O_2, N_2, or air. The UV (λ <400 nm) irradiance on the 2.5 × 5 cm^2 face was 50 mW cm^{-2}, corresponding for 3.5-eV photons to 5.3×10^{-4} einstein cm^{-2} h^{-1}, and the total flux on the 12.5-cm^2 illuminated face was 6.7×10^{-3} einstein h^{-1}. The slurry for the measurement of the rate of photodegradation of sodium 2,2-dichloropropionate (10^{-2} M in water) consisted of 150 mg of TiO_2 or Pd/TiO_2 suspended in 30 mL of water. The O_2 pressure was maintained near 1 atm. The entire UV flux was absorbed; i.e., the UV flux at the back of the cell was close to nil.

The TiO_2 used was a sample of Hombitan from Sachtleben, Hamburg, Germany. The material of 0.1–0.3-μm particle size and anatase phase was calcined at 500 °C prior to use in air. The 3 wt % Pd/TiO_2 samples were prepared by photoelectrodepositing Pd on the TiO_2 particles in an aqueous slurry (20 mL) containing $PdCl_2$ (25 mg), TiO_2 (0.5 g), and glacial acetic acid (1 mL). Following sonication, the suspension was stirred under UV illumination for 5 h. The photoelectrodeposition process involved photoassisted oxidation of acetic acid coupled with reduction of Pd^{2+} to Pd^0, a possible net reaction being[21]

$$2CH_3COOH + Pd^{2+} \xrightarrow{2h\nu} CH_3CH_3 + 2CO_2 + Pd^0 + 2H^+$$

The bluish black Pd/TiO_2 powder was thoroughly washed with deionized water, filtered off, and dried at 120 °C.

Results and Discussion

1. Negative-Charge Accumulation on TiO_2 Particles during Photooxidation of CH_3OH. That the Pd^0 catalysis observed is associated with transferring of electrons to O_2, not with a hole or $OH^\bullet$ reaction, is seen in experiments on 1.6 M methanol in water. These were performed in the cell of Figure 1, having two features. First, after the optically dense slurry is loaded into the illuminated compartment, the UV flux in the back of the compartment, where the charge-collecting glassy-carbon electrode is located, is essentially nil. Thus, the slurried particles need to traverse a distance of ~2 cm after their illumination in order to reach the nonilluminated glassy-carbon electrode. The particle transit time, determined by the rotation rate of the magnetic stirrer, is greater than 1 s. Therefore, the only charge on the particles that is observed is the charge that is not rapidly dissipated by oxidation or reduction of solution components; i.e., only long-lived electrons or holes on the particles are observed. Second, the counter/reference Ag/AgCl electrode is located in a compartment separated from the illuminated one by a frit through which TiO_2 particles could not pass. Thus, the counter-electrode reaction did not interfere with the observations of the charge of the particles in the illuminated compartment.

As will be evident from Figures 2–5, the time constants for the measured charge transfer are much smaller than those observed by Petersson, Turner, and Nozik.[23] The slow 1–3-min response of the current at the collector electrode after the onset of the illumination and the slow decay afterward in the dark are caused by the time required for the large number of particles to reach a stationary state in the period between excess charge generation during light absorption and charge gain or loss at the electrode interface, a process involving transit of the particles through the cell. The photon flux to which the particles are exposed depends on their location in the beam, varying continuously through the cell. In the experiments reported by Petersson et al.,[23] the collector electrode itself was exposed to the light beam and the particle concentration was much smaller. The fast response probably resulted from particles actually sticking to the collector electrode.

In aqueous methanol, where the initial reaction with an OH radical produces a highly reactive intermediate, electron injection, leading to current doubling, according to

$$CH_3OH + OH^\bullet \rightarrow CH_2O + H_2O + H^+ + e^- \qquad (1)$$

---

[22] Kobayashi, T.; Yoneyama, H.; Tamura, H. *J. Electrochem. Soc.* **1983**, *130*, 1706.

[23] Petersson, M. W.; Turner, J. A.; Nozik, A. J. *J. Phys. Chem.* **1991**, *95*, 221.

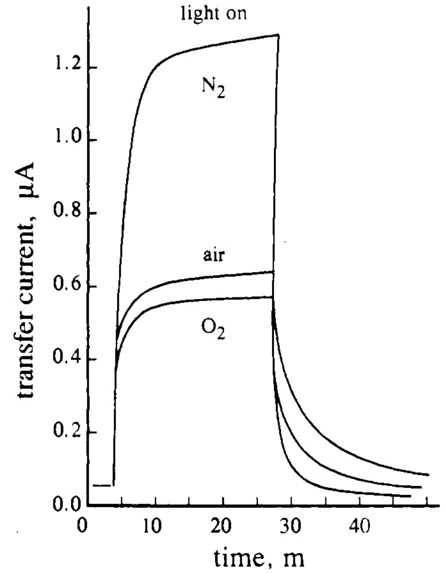

Figure 2. Delayed charge collection currents from slurried TiO_2 particles following their illumination in 1.6 M aqueous methanol solutions saturated with nitrogen, air, or oxygen. The collecting electrode was maintained at +0.35 V vs $Ag/AgCl_2$, where, as shown in Figure 4, uncharged TiO_2 particles neither gain nor lose electrons.

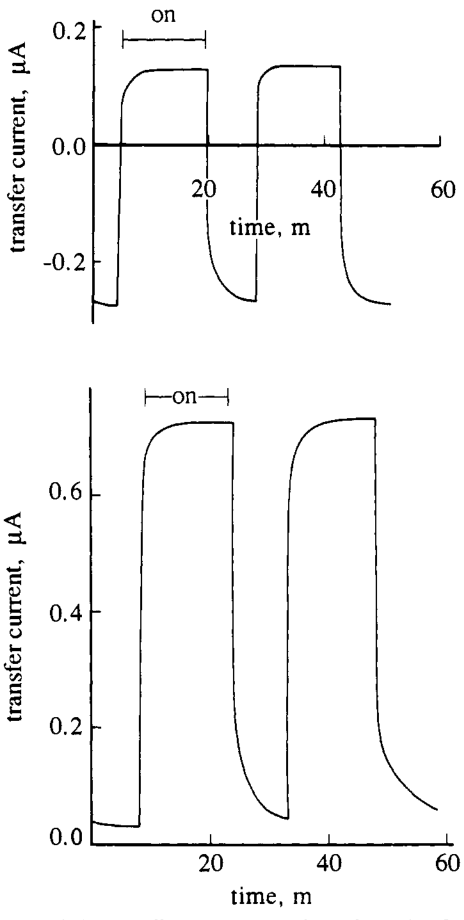

Figure 3. Delayed charge collection currents from slurried TiO_2 particles in nitrogen-saturated 1.6 M aqueous methanol at (a, top) +0.25 V and (b, bottom) +0.35 V vs Ag/AgCl. Note that following their illumination the particles are oxidized, i.e. lose electrons at either potential. However, at 0.25 V the particles pick up electrons from the electrode, while at +0.35 V they do not.

is likely. The overall single-photon-assisted oxidation reaction is

$$CH_3OH + O_2 \xrightarrow{h\nu} CH_2O + H_2O_2 \qquad (2)$$

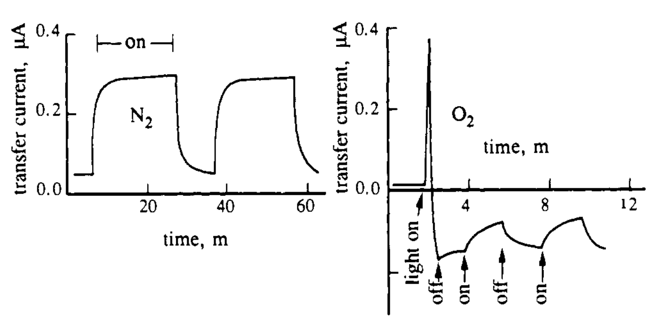

Figure 4. Palladium catalysis of the depolarization of slurried TiO_2 particles by dissolved oxygen. Delayed charge collection currents, following illumination of the particles, are shown for Pd (3 wt %) coated TiO_2 particles in nitrogen-saturated 1.6 M methanol–0.3 M NaCl (left) and in the same O_2-saturated solution (right). The charge-collecting-electrode potential is +0.35 V vs Ag/AgCl.

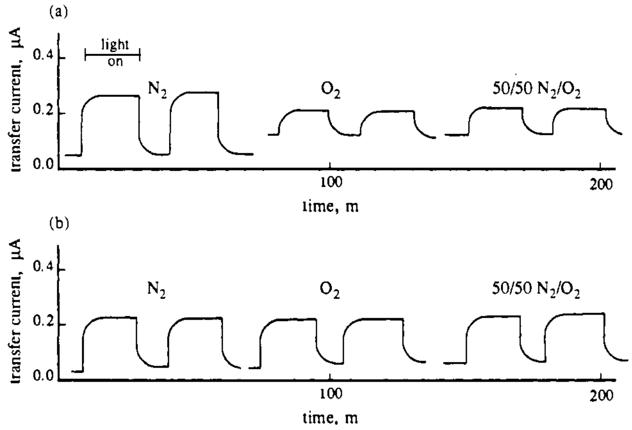

Figure 5. Dependence of the delayed charge collection current from slurried bare TiO_2 particles on the solution-saturating gas in 1.6 M aqueous methanol at 0.3 M NaCl (top) and at 3.0 M NaCl (bottom).

Figure 2 shows the current collected at the vitreous-carbon electrode when maintained at +0.35 V vs Ag/AgCl. That at this potential the TiO_2 particles are neither reduced nor oxidized in the dark is seen in Figure 3. At a potential of 0.25 V vs Ag/AgCl (Figure 3a) the TiO_2 particles are still substantially reduced in the dark; i.e., electrons are transferred from the electrode to the particles. There is no such transfer at +0.35 V vs Ag/AgCl (Figure 4b). Returning now to Figure 2, one observes under an N_2 atmosphere a substantial current when the light is on. This current is again associated with electron transfer from the TiO_2 particles to the electrode. Saturation with air lowers the current only to about half of its value under N_2, and even saturation by pure O_2 lowers it further only slightly. Thus, even in an O_2-saturated solution, the particles are substantially electron-charged because of their slow depolarization by O_2; evidently, the rate of electron transfer to O_2 does not keep up with the rate of photogeneration of holes.

In Figure 4, we see that this situation is dramatically changed when 3 wt % Pd is incorporated in the surface of the particles. Under N_2 (left) a current associated with electron transfer from the particles to the electrode still flows, but when the solution is O_2 saturated, there is no such current. The small reverse current in the presence of oxygen (electron transfer to the particles) may be caused by depletion of the particles of electrons through reduction of O_2 at the Pd catalyst. The initial anodic current spike at the first onset of illumination is apparently caused by slow processes in the dark, prior to the illumination period, which are yet to be explained. We are addressing here, however, the steady-state behavior during alternating illuminated and dark phases. We observe at steady state a slight decrease in the rate of electron transfer to the particles during the illumination period, during which electrons are photogenerated. The rate of O_2 reduction on the Pd-activated TiO_2 particles remains, however, fast enough to prevent accumulation of electrons.

This situation holds for aqueous methanol and for aqueous methanol with 0.3 M NaCl. In concentrated NaCl brines (3 M NaCl) and in the absence of Pd, the primary hole reaction is no longer generation of OH radicals. Instead, surface-adsorbed Cl atoms are generated. The adsorbed Cl atoms and Cl^- ions apparently prevent electron transfer to O_2. As a result, the current associated with electron transfer from the slurried particles to the glassy-carbon electrode is atmosphere independent, the TiO_2 particles being identically negatively charged whether under N_2, under air, or under pure O_2 (Figure 5, bottom). This, however, is not the case at lower NaCl concentrations. In 0.3 M NaCl, the current changes with the atmosphere just as it does in water in the absence of NaCl (Figure 5, top), showing that at 0.3 M NaCl the electrons are transferred to O_2.

2. Photooxidation of $CH_3CCl_2COO^-$. The effect of Pd incorporation in the TiO_2 crystallites on the rate of HCl generation through the photoassisted oxidation of 10^{-2} M sodium 2,2-dichloropropionate in water is shown in Figure 6. Pd^0 photoelectrodeposited on the particle's surface drastically increases the rate of HCl photogeneration even in amounts as small as 1 part per 10^4. Two different mechanisms for the photooxidation can be envisaged which result in different quantum yields for the production of HCl. We assume that oxidation leads to the formation of CO_2, CH_3COOH, and HCl and is compensated by the reduction of O_2 to H_2O_2. If we neglect the apparently much slower further oxidation of acetic acid and processes in which H_2O_2 may be involved (photocatalytic decomposition and oxidation of CH_3COOH), then the net reaction is

$$CH_3CCl_2COO^- + O_2 + 2H_2O + xh\nu \rightarrow CH_3COOH + CO_2 + H^+ + 2Cl^- + H_2O_2 \quad (3)$$

The number of photons, x, can be 1 or 2, depending on whether (a) each of the two oxidation steps requires a photon or (b) the second step occurs spontaneously, resulting from injection of an electron into the semiconductor, i.e. involving photocurrent doubling, well-known in the photooxidation of some organic molecules on semiconductors, including TiO_2.[24-29] The possible reaction sequences (eqs 4-7) are the following:

Sequence A

$$h\nu \rightarrow h^+ + e^- \quad (4a)$$

$$h^+ + H_2O \rightarrow {}^{\bullet}OH + H^+ \quad (5a)$$

$${}^{\bullet}OH + CH_3CCl_2COOH + H_2O \rightarrow CH_3COOH + CO_2 + 3H^+ + 2Cl^- + e^- \quad (6a)$$

$$O_2 + 2e^- + 2H^+ \rightarrow H_2O_2 \quad (7a)$$

This sequence results in $x = 1$. The apparent quantum yield for HCl production is in this case 2, while the primary yield is 1.

Sequence B

$$2h\nu \rightarrow 2h^+ + 2e^- \quad (4b)$$

$$2h^+ + 2H_2O \rightarrow 2{}^{\bullet}OH + 2H^+ \quad (5b)$$

$$2{}^{\bullet}OH + CH_3CCl_2COOH \rightarrow CH_3COOH + CO_2 + 2H^+ + 2Cl^- \quad (6b)$$

$$O_2 + 2e^- + 2H^+ \rightarrow H_2O_2 \quad (7b)$$

In this sequence, $x = 2$ and the primary quantum yield for the generation of ${}^{\bullet}OH$ radicals is the same as the apparent yield for HCl production.

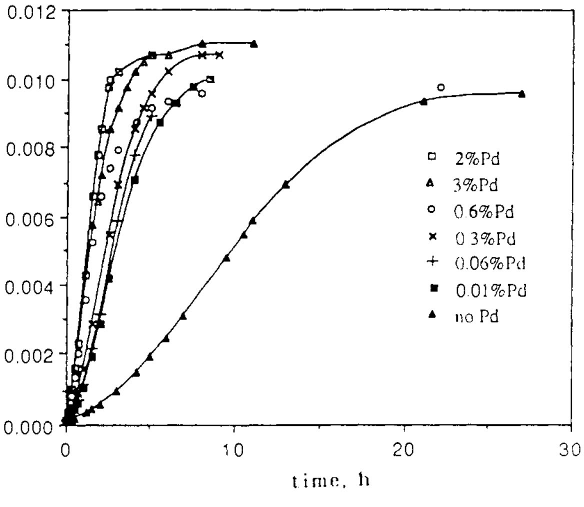

Figure 6. Cocatalysis of the photoassisted oxidation of 10 mM sodium 2,2-dichloropropionate: dependence of the rate of HCl generation on the Pd loading of the TiO_2 particles.

Table I. Effect of Incorporating Pd^0 in the Slurried TiO_2 Particles on the Efficiency of the Photoassisted Oxidation of 10^{-2} M Sodium 2,2-Dichloropropionate by Oxygen

% Pd	rate of H^+ evol, 10^{-3} mol h^{-1}	act quant eff	prim quant eff for sequence A
0.00	0.67	0.20	0.10
0.01	2.2	0.64	0.32
0.06	2.4	0.70	0.35
0.3	2.6	0.78	0.39
0.6	3.4	1.02	0.51
2.0	4.8	1.44	0.72
3.0	3.9	1.16	0.58

The results of Figure 6 are analyzed for the initial quantum yield in Table I. Since the apparent yield exceeds a quantum efficiency of 1 in the best results, Sequence A must be the dominating mechanism. Step 6a may include the following individual reactions:

$$CH_3CCl_2COOH + {}^{\bullet}OH \rightarrow CH_3CCl_2 + CO_2 + H_2O \quad (8)$$

$$CH_3CCl_2 + H_2O \rightarrow CH_3COCl + Cl^- + 2H^+ + e^- \quad (9)$$

$$CH_3COCl + H_2O \rightarrow CH_3COOH + H^+ + Cl^- \quad (10)$$

The highest primary quantum efficiency obtained in our experiments is 0.72. Losses are caused by recombination at the surface and at the metal particles, as well as by reverse reactions of electrons with ${}^{\bullet}OH$ radicals. The catalytic or quantum efficiency of photoassisted oxidation is increased by Pd deposits on the TiO_2 particles by a factor of 7 at a Pd content of 2%. The efficiency decreases at higher Pd loadings.

We note that monolayer Pd coverage of 0.2-μm-diameter TiO_2 particles corresponds to a loading of 1.8 wt %. Thus the best efficiency is reached approximately at about monolayer equivalent coverage. The deposited Pd^0 will not form a monolayer but will aggregate to clusters, leaving much of the surface available for oxidation of adsorbed H_2O by holes. Excessive coverage promotes, however, recombination. This explains the decrease in efficiency at higher loading of Pd. At very low coverage, corresponding to $^1/_{200}$th of a monolayer, the quantum efficiency is tripled.

While Pd^0 catalysis of the photoassisted oxidation of 2,2-dichloropropionate by oxygen is evident, a note of caution is required in the quantitative interpretation of the data. Okamoto et al.[30] found that the photocatalytic activity of TiO_2 is pH dependent. Specifically, they reported for anatase an increase by a factor of 1.5 in the rate of photoassisted oxidation of phenol when the pH drops from 6.5 to 3.5. With the concentration of HCl increasing in our experiments from $\sim 10^{-3}$ to $\sim 10^{-2}$ M, the rates and

---

(24) Morrison, S. R.; Freund, T. *J. Chem. Phys.* **1967**, *47*, 1543.

(25) Gerischer, H. *Surf. Sci.* **1969**, *18*, 17.

(26) Manirannan, A.; Fujishima, A.; Subba Rao, G. V. *Ber. Bunsen-Ges. Phys. Chem.* **1988**, *92*, 1522.

(27) Harima, Y.; Morrison, S. R. *J. Electroanal. Chem. Interfacial Electrochem.* **1987**, *220*, 173.

(28) Nosaka, Y.; Sasaki, H.; Norimatsu, K.; Miyama, H. *Chem. Phys. Lett.* **1984**, *105*, 456.

(29) Maeda, Y.; Fujishima, A.; Honda, K.; *J. Electrochem. Soc.* **1981**, *128*, 1731.

(30) Okamoto, K.; Yamamoto, Y.; Tanaka, H.; Tanaka, M.; Itaya, A. *Bull. Chem. Soc. Jpn.* **1985**, *58*, 2015.

quantum efficiencies of Table I are averaged values over a pH range between 3 and 2 and their accuracy is ±20%. Nevertheless, because in all of our measurements the change in pH has been the same, the relative quantum efficiencies are quite accurate.

Acknowledgment. We thank Prof. James R. Brock and Prof. John G. Ekerdt for useful discussions and Mrs. Maya Nair for competent assistance. This work was supported by the Division of advanced Energy Projects, Office of Basic Energy Sciences, U.S. Department of Energy, under Contract DE-FG05-90ER12101-A0002.

Registry No. CH_3OH, 67-56-1; Pd, 7440-05-3; TiO_2, 13463-67-7; O_2, 7782-44-7; sodium 2,2-dichloropropionate, 127-20-8.

Characterization of the Energy Surface for the Oxidative Addition of Silanes to $CpMn(CO)_2$(heptane)

Dennis M. Hester, Jiemin Sun, Aaron W. Harper, and Gilbert K. Yang*

Contribution from the Department of Chemistry, University of Southern California, Los Angeles, California 90089-0744. *Received November 13, 1991*

Abstract: The energetic surface for the oxidative addition reaction of silanes to $CpMn(CO)_2$(heptane) (**2**) has been studied by a combination of photoacoustic calorimetry and variable-temperature kinetic studies. For seven different silanes the enthalpy for the oxidative addition reaction, ΔH_{-1}, ranged from −22.1 to −13.5 kcal/mol. ΔH_{-1} was found to depend both on the electron donating ability of the silane as well as on the cone angle of the silane. A threshold cone angle of 135° must be reached before the steric effects turn on. The rate constants for the oxidative addition reactions at 25 °C were all similar, ca. 2.5×10^6 L/(mol·s), indicative of an early transition state where steric and electronic effects have not yet manifested themselves. Kinetic studies of the reductive elimination of Et_3SiH from $CpMn(CO)_2(H)(Et_3Si)$ are consistent with a mechanism involving a pre-equilibrium step with the reactive intermediate **2** which is then trapped by PPh_3. The activation parameters are the following: $\Delta H_1^{\ddagger} = 27.4 \pm 0.8$ kcal/mol and $\Delta S_1^{\ddagger} = 11.5 \pm 2.5$ eu. The values for $\Delta H_{-1}^{\ddagger}$ determined by Wrighton and the results of $\Delta H_1^{\ddagger}$ and ΔH_{-1} reported here are consistent with one another. Trapping of the $CpMn(CO)_2$(heptane) intermediate is favored by PPh_3 over Et_3SiH with $\Delta\Delta H^{\ddagger} = -2.1 \pm 0.5$ kcal/mol and $\Delta\Delta S^{\ddagger} = -2.7 \pm 1.0$ eu. From the values of $\Delta H_{-1}^{\ddagger}$ and $\Delta H_1^{\ddagger}$, the strength of the Mn–heptane interaction is estimated to be 8 kcal/mol.

The oxidative addition of alkylsilanes to transition-metal complexes has been the focus of much recent attention.[1] This reaction plays an integral role in the hydrosilation of olefins and serves as an important model for understanding analogous C–H activation reactions. The bonding in metal silyl hydride complexes varies in description from being a relatively weak η^2-silane–metal interaction at one extreme to the stronger oxidative addition interaction found in a true metal silyl hydride moiety. From the relative rates of reductive elimination of Cl_3SiH and Ph_3SiH from the corresponding $CpMn(CO)_2(H)(SiR_3)$ complexes, Graham and Hart-Davis[2] concluded that "Cl_3SiH is much more firmly attached" to the complex than is Ph_3SiH. This observation is now understood to be a result of more advanced Si–H bond cleavage with the more electron deficient Cl_3SiH. Data from single-crystal X-ray and neutron diffraction analyses[3] and UV photoelectron spectra[4] support the conclusion that the interaction of the silane with the Mn center more closely approaches complete oxidative addition when more electron withdrawing substituents are on the silane. These results are also supported by theoretical studies which show that an important component of the silane–metal interaction is π-back-bonding from the $CpMn(CO)_2$ moiety to the Si–H σ^* orbital.[5] Electron-withdrawing substituents on the silane will lead to a stronger silane–metal interaction.

In contrast, Zhang, Dobson, and Brown[6] have published recent work which suggests that more electron donating substituents on the silane result in stronger Cr–silane interactions. This result is thought to be a consequence of the greater role of σ-donation from the silane to the electrophilic $Cr(CO)_5$ center (in comparison to $CpMn(CO)_2$). These workers also found that the rate of the reductive elimination of silane from $(CO)_5Cr(H)(SiRR'_2)$ could be described as a function of both the electron donating ability and the cone angle of the corresponding phosphine.

Comparatively little is known about how the steric requirements of the silane influence the nature of the metal–silane interaction in the $CpMn(CO)_2(H)(SiR_3)$ system. Wrighton and Hill have reported kinetic studies of the oxidative addition reaction of silanes to $CpMn(CO)_2$ in hydrocarbon solution.[7] A slight dependence on the steric bulk of the silane was found. In this paper we present studies of the heat of reaction of coordinatively unsaturated $CpMn(CO)_2$(heptane) with silanes of differing steric bulk. A strong dependence on steric bulk is found for silanes exceeding a "steric threshold", but little effect is seen for smaller silanes. The kinetics of both the oxidative addition process and the reductive elimination process are discussed in the context of the enthalpy of reaction. The stabilization of the $CpMn(CO)_2$ moiety by the heptane solvent can be inferred from these data. Together, a complete picture of the Mn–silane energy profile is presented.

Experimental Section

General. Ferrocene (Aldrich) was sublimed before use and $CpMn(CO)_3$ (Strem) was recrystallized prior to use. Heptane was distilled

---

(1) For a recent review see: Schubert, U. *Adv. Organomet. Chem.* **1990**, *30*, 151–187.

(2) Hart-Davis, A. J.; Graham, W. A. G. *J. Am. Chem. Soc.* **1971**, *93*, 4388–4393.

(3) (a) Schubert, U.; Scholz, G.; Müller, J.; Ackermann, K.; Worle, B.; Stansfield, R. F. D. *J. Organomet. Chem.* **1986**, *306*, 303. (b) Graham, W. A. G. *J. Organomet. Chem.* **1986**, *300*, 81. (c) Carrē, F.; Colomer, E.; Corriu, R. J. P.; Vioux, A. *Organometallics* **1984**, *3*, 1272. (d) Graham, W. A. G.; Bennett, M. J. *Chem. Eng. News* **1970**, *48(24)*, 75. (e) Schubert, U.; Ackermann, K.; Worle, B. *J. Am. Chem. Soc.* **1982**, *104*, 7378. (f) Schubert, U.; Ackermann, K.; Kraft, G.; Worle, B. *Z. Naturforsch. B: Anorg. Chem. Org. Chem.* **1983**, *38*, 1488.

(4) (a) Lichtenberger, D. L.; Rai-Chaudhuri, A. *J. Am. Chem. Soc.* **1989**, *111*, 3583. (b) Lichtenberger, D. L.; Rai-Chaudhuri, A. *J. Am. Chem. Soc.* **1990**, *112*, 2492. (c) Lichtenberger, D. L.; Rai-Chaudhuri, A. *Inorg. Chem.* **1990**, *29*, 975.

(5) Rabaã, H.; Saillard, J.-Y.; Schubert, U. *J. Organomet. Chem.* **1987**, *330*, 397–413.

(6) Zhang, S.; Dobson, G. R.; Brown, T. L. *J. Am. Chem. Soc.* **1991**, *113*, 6908–6916.

(7) Hill, R. H.; Wrighton, M. S. *Organometallics* **1987**, *6*, 632–638.

0002-7863/92/1514-5234$03.00/0